

# Electroweak production of light scalar-pseudoscalar pairs from extended Higgs sectors

Rikard Enberg<sup>a</sup>, William Klemm<sup>a,b</sup>, Stefano Moretti<sup>c</sup>, Shoaib Munir<sup>d</sup>

<sup>a</sup>*Department of Physics and Astronomy, Uppsala University, Box 516, SE-751 20 Uppsala, Sweden*

<sup>b</sup>*School of Physics & Astronomy, University of Manchester, Manchester M13 9PL, UK*

<sup>c</sup>*School of Physics & Astronomy, University of Southampton, Southampton SO17 1BJ, UK*

<sup>d</sup>*School of Physics, Korea Institute for Advanced Study, Seoul 130-722, Republic of Korea*

---

## Abstract

In models with extended Higgs sectors, it is possible that the Higgs boson discovered at the LHC is not the lightest one. We show that in a realistic model (the Type I 2-Higgs Doublet Model), when the sum of the masses of a light scalar and a pseudoscalar ( $h$  and  $A$ ) is smaller than the  $Z$  boson mass, the Electroweak (EW) production of an  $hA$  pair can dominate over QCD production by orders of magnitude, a fact not previously highlighted. This is because in the  $gg$ -initiated process,  $hA$  production via a resonant  $Z$  in the  $s$ -channel is prohibited according to the Landau-Yang theorem, which is not the case for the  $q\bar{q}$ -initiated process. We explore the parameter space of the model to highlight regions giving such  $hA$  solutions while being consistent with all constraints from collider searches,  $b$ -physics and EW precision data. We also single out a few benchmark points to discuss their salient features, including the  $hA$  search channels that can be exploited at Run II of the LHC.

---

## 1. Introduction

Most models for physics beyond the Standard Model (SM) predict extended Higgs sectors, with additional Higgs (pseudo)scalars. Two-Higgs Doublet Models (2HDMs), which contain two Higgs doublets  $\phi_1$  and  $\phi_2$  (see [1] for a review), are among the simplest non-trivial extensions of the SM. The Higgs sector of a CP-conserving 2HDM contains three neutral Higgs bosons, two scalars and a pseudoscalar ( $h$ ,  $H$ , with  $m_h < m_H$ , and  $A$ , respectively), and a charged pair  $H^\pm$ . One of the two CP-even Higgs bosons must have properties consistent with the observed 125 GeV state [2, 3, 4],  $H_{\text{obs}}$ . At the Large Hadron Collider (LHC), the neutral Higgs bosons of a 2HDM can be produced both singly, dominantly via gluon fusion, and in identical or mixed pairs. We discuss here a scenario in which the  $h$  and  $A$  states of the Type-I 2HDM (2HDM-I),<sup>1</sup> with masses satisfying  $m_h + m_A < M_Z$ , can pass the present experimental constraints from the Large Electron Positron (LEP) collider, the Tevatron and the LHC, with the heavier  $H$  state being identified with  $H_{\text{obs}}$ .

The LHC is a hadron collider that can yield collisions with very small momentum fraction  $x$  of the scattered partons and very large squared momentum transfer  $Q^2$ . Because the proton has a large gluon density at small  $x$ , one would hope to initiate  $Z$  production from gluon-gluon ( $gg$ ) scattering (see the left diagram of Fig. 1a), with the  $hA$  final state produced from  $Z$  decay. However, owing to the

Landau-Yang theorem [5, 6],  $gg$  can only scatter via a  $Z$  if it is non-resonant (i.e., off-shell, denoted by  $Z^*$ ) [7]. This leads to a much depleted cross section for the  $hA$  signal and, additionally, to the inability of using  $Z$  mass reconstruction from the invariant mass of the  $hA$  (visible) decay products for suppressing backgrounds. In the case of the tree-level quark-antiquark ( $q\bar{q}$ )-initiated process, however, the  $Z$  boson can be produced on-shell (left diagram of Fig. 1b). The  $hA$  final state can also be produced from double Higgs-strahlung off heavy quarks (i.e.,  $b$ - and  $t$ -quarks), at the one-loop level (right diagram of Fig. 1a) and at the tree level (right diagram of Fig. 1b), in the case of  $gg$  and  $q\bar{q}$  collisions, respectively.

It is the purpose of this Letter to highlight the hitherto neglected predominance of the  $q\bar{q}$ -initiated tree-level production of a light  $hA$  pair at the LHC with respect to the  $gg$ -initiated one-loop production in a Type-I 2HDM. (See Ref. [8] for higher order QCD corrections to the corresponding diagrams.) We additionally outline the region of the 2HDM-I parameter space where the former can be accessed above and beyond the yield of the latter and present benchmark points to serve as a guideline for probing this production process at the current LHC run.

## 2. Model, parameter scan and constraints

In general, in a 2HDM, depending on how the two doublets couple to fermions, Flavor Changing Neutral Currents (FCNCs) can be mediated by (pseudo)scalars at the tree level. The requirement of vanishing FCNCs thus puts

---

<sup>1</sup>In the Type I model, all fermions get mass from Yukawa couplings to only one of the doublets, see below.

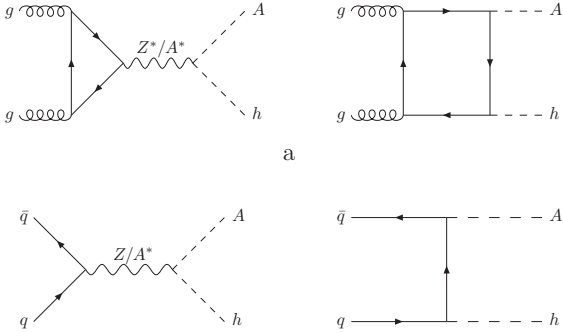


Figure 1: Diagrams contributing to (a) QCD production and (b) EW production of the  $hA$  pair.

very strong restrictions on the coupling matrices. The simplest way to avoid large FCNCs is to impose a  $Z_2$  symmetry so that each type of fermion only couples to one of the doublets (“natural flavor conservation”) [9, 10]. There are four basic ways of assigning the  $Z_2$  charges, and here we consider the case where only the doublet  $\phi_2$  couples to all fermions, known as the Type I model. The Higgs potential for the CP-conserving 2HDM-I is written as

$$\begin{aligned}
V &= m_{11}^2 \phi_1^\dagger \phi_1 + m_{22}^2 \phi_2^\dagger \phi_2 - [m_{12}^2 \phi_1^\dagger \phi_2 + \text{h.c.}] \\
&+ \frac{1}{2} \lambda_1 (\phi_1^\dagger \phi_1)^2 + \frac{1}{2} \lambda_2 (\phi_2^\dagger \phi_2)^2 + \lambda_3 (\phi_1^\dagger \phi_1) (\phi_2^\dagger \phi_2) \\
&+ \lambda_4 (\phi_1^\dagger \phi_2) (\phi_2^\dagger \phi_1) + [\frac{1}{2} \lambda_5 (\phi_1^\dagger \phi_2)^2 + \text{h.c.}], \quad (1)
\end{aligned}$$

which is invariant under the symmetry  $\phi_1 \rightarrow -\phi_1$  up to the soft breaking term proportional to  $m_{12}^2$ . Through the minimization conditions of the potential,  $m_{11}^2$  and  $m_{22}^2$  can be traded for the vacuum expectation values,  $v_1$  and  $v_2$ , of the two Higgs fields and the tree-level mass relations allow the quartic couplings  $\lambda_{1-5}$  to be substituted by the four physical Higgs boson masses and the neutral sector term  $s_{\beta-\alpha}$  (short for  $\sin(\beta - \alpha)$ , with the angle  $\beta$  defined through  $\tan \beta = v_2/v_1$ ), where  $\alpha$  mixes the CP-even Higgs states.

In order to test the consistency of solutions with  $m_h + m_A < M_Z$  in the 2HDM-I with the most crucial and relevant theoretical and experimental constraints (listed further below), we performed a scan of its parameter space<sup>2</sup> using 2HDMC-v1.7.0 [12]. The (randomly) scanned ranges of the free parameters (with  $m_H = 125$  GeV) are given in the second column of Tab. 1. Because only a select region of the parameter space is allowed by current constraints, we used the distributions resulting from this initial scan to determine the most relevant parameter ranges, which we focused on in a second scan, shown in the rightmost column of Tab. 1.

<sup>2</sup>Note that a similar region of parameter space was captured by Ref. [11]

Parameter	Initial range	Refined range
$m_h$ (GeV)	(10, 80)	(10, $2M_Z/3$ )
$m_A$ (GeV)	(10, $M_Z - m_h$ )	( $m_h/2$ , $M_Z - m_h$ )
$m_{H^\pm}$ (GeV)	(90, 500)	(90, 150)
$s_{\beta-\alpha}$	(-1, 1)	(-0.25, 0)
$m_{12}^2$ (GeV <sup>2</sup> )	(0, $m_A^2 \sin \beta \cos \beta$ )	(0, $m_A^2 \sin \beta \cos \beta$ )
$\tan \beta$	(2, 25)	(-0.95, -1.1)/ $s_{\beta-\alpha}$

Table 1: 2HDM-I parameters and their scanned ranges.

During the scan, each sampled model point was subjected to the following conditions:

- Unitarity, perturbativity, and vacuum stability enforced through the default 2HDMC method.
- Consistency at 95% Confidence Level (CL) with the experimental measurements of the oblique parameters  $S$ ,  $T$  and  $U$ , again, calculated by 2HDMC. We compare these to the fit values [13],  $S = 0.00 \pm 0.08$  and  $T = 0.05 \pm 0.07$ , in an ellipse with a correlation of 90%. All points further satisfy  $U = 0.05 \pm 0.10$ .
- Satisfaction of the 95% CL limits on  $b$ -physics observables calculated with the public code SuperIso-v3.4 [14].
- Consistency with the  $Z$  width measurement from LEP,  $\Gamma_Z = 2.4952 \pm 0.0023$  GeV [13]. The partial width  $\Gamma(Z \rightarrow hA)$  was required to fall within the  $2\sigma$  experimental uncertainty of the measurement.
- Consistency of the mass and signal rates of  $H$  with the LHC data on  $H_{\text{obs}}$ . The combined 68% CL results from ATLAS and CMS for the most sensitive channels are [15]:  $\mu_{ggF+t\bar{t}H}^{\gamma\gamma} = 1.15_{-0.25}^{+0.28}$ ,  $\mu_{\text{VBF}+VH}^{\gamma\gamma} = 1.17_{-0.53}^{+0.58}$ ,  $\mu^{4\ell} = 1.40_{-0.25}^{+0.30}$ . We required that the equivalent quantities, calculated with HiggsSignals-v1.3.2 [16], satisfy these measurements at 95% CL, assuming Gaussian uncertainties.
- Consistency of all Higgs states with the direct search constraints from LEP, Tevatron, and LHC at the 95% CL tested using the public tool HiggsBounds-v4.3.1 [17, 18, 19, 20].

The points were also required to satisfy some additional constraints from LEP and LHC that have not (yet) been implemented in HiggsBounds. Consistency with the combined LEP  $H^\pm$  searches in the 2HDM-I [21] was ensured by requiring that  $m_{H^\pm} > 90$  GeV. The LEP-II constraints on  $e^+e^- \rightarrow \gamma\gamma b\bar{b}$  [22] were also taken into account. While these constraints are mass dependent, we conservatively required  $\cos^2(\beta - \alpha) \text{BR}(h \rightarrow \gamma\gamma) \text{BR}(A \rightarrow b\bar{b}) < 0.02$ . Moreover, the results of the  $\mu\mu\tau\tau$  final state studies performed by ATLAS [23] as well as of the  $\tau\tau\tau\tau$  [24],  $\mu\mu\tau\tau$  [25] and  $\mu\mu b\bar{b}$  [26] analyses from CMS were tested against.

### 3. Scan results

From the output of our initial scan, we noticed that the LHC observation of a very SM-like  $H_{\text{obs}}$  pushes the model towards the alignment limit,  $s_{\beta-\alpha} \rightarrow 0$ . Addition-

ally, strong constraints from LEP searches lead to suppressed  $h/A$  couplings to fermions,<sup>3</sup> producing a strong correlation  $s_{\beta-\alpha} \approx -1/\tan\beta$ . We also find that a relatively light charged Higgs ( $m_{H^\pm} \lesssim 120$  GeV) is necessary, as a charged Higgs mass too far separated from  $m_h$  or  $m_A$  results in large contributions to the  $T$ -parameter.<sup>4</sup> Existing searches for charged Higgs bosons in this mass range typically focus on production from top decays followed by charged Higgs boson decays to either  $\tau\nu$  or  $cs$ . For the points selected by the scan, these branching ratios typically fall below the percent level, in many cases by several orders of magnitude, with maximal values of  $\text{BR}(t \rightarrow H^+b) \lesssim 0.04$ ,  $\text{BR}(H^+ \rightarrow \tau^+\nu_\tau) \lesssim 0.01$ , and  $\text{BR}(H^+ \rightarrow c\bar{s}) \lesssim 6 \times 10^{-3}$ . This places them well below existing constraints, including recent LHC results [27, 28, 29] not yet included in HiggsBounds. Instead of the standard decays, the low masses of  $h$  and  $A$  in the scenario considered here allow the  $H^\pm$  to decay dominantly in the  $W^*h$  or  $W^*A$  channels (with the respective branching ratios alternatively near unity), which have not yet been examined at the LHC.<sup>5</sup>

Numerous constraints restrict the possible masses of  $h$  and  $A$ . In Fig. 2 we show the points passing all the constraints mentioned above in the  $(m_h, m_A)$  plane. Because the  $hAZ$  coupling is maximized in the favored  $s_{\beta-\alpha} \rightarrow 0$  limit, the constraint from  $\Gamma_Z$ , the  $1\sigma$  and  $2\sigma$  contours for which are also shown, is particularly severe. We note two distinct regions with a large density of points in the figure. The region near the top left corner corresponds to the  $m_A > m_h$  (heavier  $A$ ) scenario. This region cuts off sharply at  $m_A = m_H/2$  due to the possibility of the  $H \rightarrow AA$  decay arising, which potentially leads to a suppression of the signal strengths for the SM-like  $H$  (for the 2HDM-I scenarios we consider, these signal strengths are always below 1 to begin with). This possibility can be avoided with a sufficiently suppressed  $HAA$  coupling, as a result of which additional points satisfying all constraints appear in the region corresponding to the  $m_h > m_A$  (heavier  $h$ ) scenario near the lower right corner of the figure. When  $m_h > 2m_A$ , the  $h \rightarrow AA$  decay channel opens up, and the model is severely constrained by LEP searches for processes such as  $e^+e^- \rightarrow hA \rightarrow (AA)A \rightarrow (b\bar{b}b\bar{b})b\bar{b}$  [31]. Consequently, we did not find acceptable points with  $m_h > 2m_A$ .

The color map in Fig. 2 depicts the total cross section for the  $q\bar{q}' \rightarrow hA$  process, which evidently grows larger as one moves away from the diagonal and  $m_h + m_A$  gets smaller. For calculating this cross section, we used the 2HDMC model [12] with MadGraph5\_aMC@NLO [32], considering both 4- ( $q = u, d, c, s$ ) and 5- ( $q = u, d, c, s, b$ )

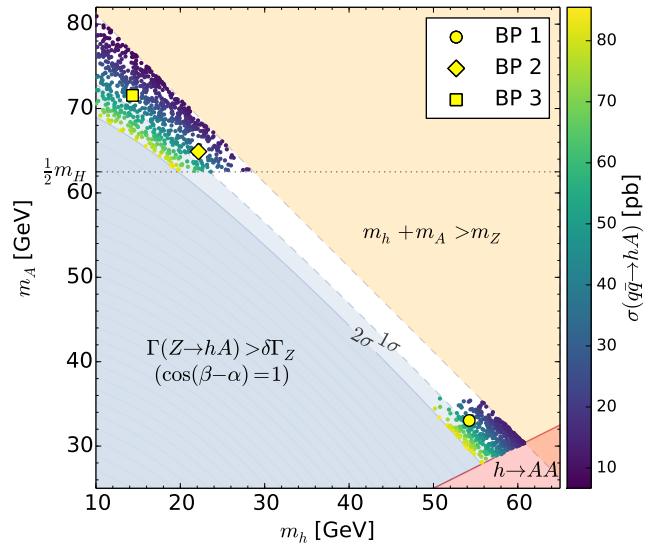


Figure 2: Constraints and accepted points in the  $(m_h, m_A)$  plane. Shaded areas: Red –  $m_h > 2m_A$ , allowing  $h \rightarrow AA$  decays; Blue – theoretical prediction of the  $Z \rightarrow hA$  partial width exceeds experimental uncertainty at the  $1\sigma$  (lighter) and  $2\sigma$  (darker) levels, in the limit  $\cos(\beta - \alpha) = 1$ ; Orange –  $m_h + m_A$  above the  $m_Z$  threshold, not considered in this study. The color map corresponds to the total cross section for the  $q\bar{q}' \rightarrow hA$  process at  $\sqrt{s} = 13$  TeV, and the three benchmark points have been highlighted in yellow.

flavor schemes. The 5-flavor scheme predictions differ by less than 3% from those of the 4-flavor one due to the small  $b$ -quark couplings. Also highlighted in the figure are the three Benchmark Points (BPs) selected to demonstrate the typical characteristics of the interesting parameter space regions. These BPs will be discussed in detail later.

#### 4. EW vs. QCD production

In order to be able to compare the relative strengths of the  $q\bar{q}' \rightarrow hA$  production mode and the  $gg \rightarrow hA$  mode, we also calculated the cross section for the latter for each point using codes developed with MadGraph5\_aMC@NLO [32] for Higgs pair production [33]. The comparison is shown in Fig. 3, where one notices that the maximal cross section achievable for QCD production is about three orders of magnitude smaller than that for EW production, which can reach as high as  $\sim 90$  pb. Also, for the points shown, while the maximal cross section for EW production is consistent across the two  $(m_h, m_A)$  regions, which can be distinguished through the color map in  $m_A$ , QCD production clearly prefers the heavier  $A$  scenario.

#### 5. Benchmarks

The input parameters for the three BPs shown in Fig. 2 are given in Tab. 2 along with the corresponding cross sections in the two  $hA$  production channels analyzed. BP1

<sup>3</sup>In the 2HDM-I, the couplings of  $h$  and  $A$  to fermions go as  $g_{hf\bar{f}} \sim \cos\alpha/\sin\beta$  and  $g_{Af\bar{f}} \sim \pm \cot\beta$ .

<sup>4</sup>This requirement of a light charged Higgs prevents us from finding similar points in Type-II models, where a higher  $m_{H^\pm}$  is required by  $B$ -physics constraints.

<sup>5</sup>These decay modes of the  $H^\pm$  will be discussed further in [30].

BP	$m_h$	$m_A$	$m_{H^\pm}$	$s_{\beta-\alpha}$	$m_{12}^2$	$\tan\beta$	$\sigma(q\bar{q})$	$\sigma(gg)$
1	54.2	33.0	95.9	-0.12	118.3	9.1	41.2	$1.5 \times 10^{-4}$
2	22.2	64.9	101.5	-0.05	10.6	22.1	34.4	$7.2 \times 10^{-3}$
3	14.3	71.6	107.2	-0.06	2.9	16.3	31.6	$1.1 \times 10^{-2}$

Table 2: Input parameters and parton-level cross sections (in pb) corresponding to the selected benchmark points. All masses are in GeV and for all points  $m_H = 125$  GeV.

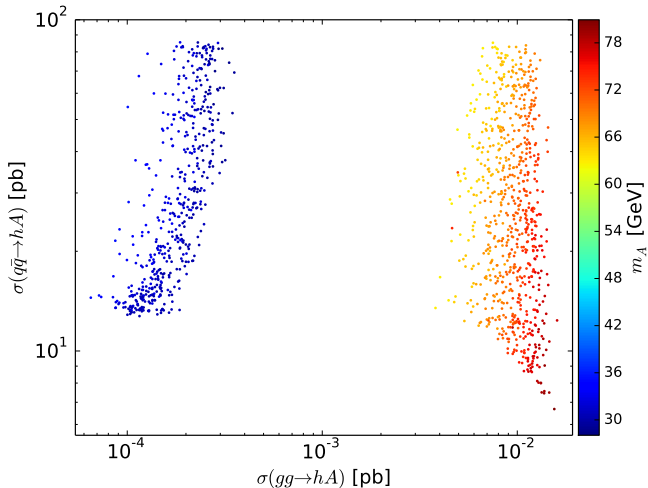


Figure 3: Cross sections for  $q\bar{q}$ - vs.  $gg$ -initiated  $hA$  production at the LHC with  $\sqrt{s} = 13$  TeV, for points satisfying all the constraints described in the text. The color map indicates  $m_A$ .

corresponds to the heavier  $h$  scenario while BP2 and BP3 correspond to the heavier  $A$  scenario.

In Tab. 3 we list the BRs of  $h$  and  $A$  in the most important decay channels for each BP. The allowed points in the heavier  $h$  scenario all have characteristics similar to BP1 – a highly fermiophobic  $h$  which consequently decays dominantly to  $Z^*A$  and a light  $A$  which decays primarily into pairs of third generation fermions.<sup>6</sup> The main signatures of interest would then include  $Z^*b\bar{b}b\bar{b}$ ,  $Z^*b\bar{b}\tau\tau$ , and  $Z^*\tau\tau\tau\tau$ . A similar situation is also possible in the heavier  $A$  scenario, as seen for BP2, where the roles of  $A$  and  $h$  are now reversed, but the most common final states remain the same. Unlike  $A$ , however, the light  $h$  can also decay dominantly to two photons (due to contribution from  $W^\pm$  loops, which is missing in the  $A \rightarrow \gamma\gamma$  decay), thus opening up the possibility of  $Ah \rightarrow (Z^*h)h \rightarrow Z^*\gamma\gamma\gamma\gamma$  or  $Z^*\gamma\gamma b\bar{b}$  decay chain for points like BP3.

## 6. Concluding remarks

In summary, we have shown that, even when the most up-to-date theoretical and experimental constraints are

<sup>6</sup>The  $h \rightarrow Z^*A$  and  $A \rightarrow Z^*h$  decays were previously discussed in a fermiophobic model in [34].

BP	BR( $h \rightarrow \dots$ ) [%]				BR( $A \rightarrow \dots$ ) [%]		
	$Z^*A$	$b\bar{b}$	$\gamma\gamma$	$\tau\tau$	$Z^*h$	$b\bar{b}$	$\tau\tau$
1	<b>94</b>	5	< 1	< 1	0	<b>86</b>	7
2	0	<b>83</b>	3	7	<b>86</b>	12	1
3	0	<b>60</b>	<b>24</b>	7	<b>90</b>	8	1

Table 3: Dominant BRs [%] of  $h$  and  $A$  for the BPs. BRs greater than 20% are highlighted in bold.

imposed, the 2HDM-I offers an intriguing phenomenological situation wherein  $m_h + m_A < m_Z$ . This possibility is precluded in other 2HDM Types. Such  $hA$  pairs can be produced in  $q\bar{q}$ -annihilation via resonant  $Z$  in the  $s$ -channel, unlike the case of  $gg$  fusion, where their production can only proceed via non-resonant  $Z^*$ , owing to the Landau-Yang theorem. As a consequence, at the LHC Run II, the former would yield event rates up to four orders of magnitude larger than the latter. Taking into account also the double Higgs-strahlung production, the inclusive rates for the  $q\bar{q} \rightarrow hA$  process can be as large as tens of pb, and hence amenable to experimental investigation and potential discovery by the LHC *already at present*.

Finally, to demonstrate their feasibility, we have provided a few 2HDM-I parameter configurations producing distinctive  $hA$  decay patterns. We look forward to the ATLAS and CMS experiments testing this hitherto neglected scenario against their data, as establishing one or more of the potential  $hA$  signatures discussed here will provide not only a direct proof of a non-minimal Higgs sector but also circumstantial evidence of a specific 2HDM structure.

## Acknowledgments

The work of RE and SMO is funded through the grant H2020-MSCA-RISE-2014 No. 645722 (NonMinimalHiggs). SMO is supported in part through the NExT Institute and STFC Consolidated Grant ST/J000396/1. This work is also supported by the Swedish Research Council under contract 621-2011-5107.

## References

## References

- [1] G. Branco, P. Ferreira, L. Lavoura, M. Rebelo, M. Sher, et al., Theory and phenomenology of two-Higgs-doublet models, Phys. Rept. 516 (2012) 1–102. [arXiv:1106.0034](https://arxiv.org/abs/1106.0034), doi:10.1016/j.physrep.2012.02.002.

- [2] G. Aad, et al., Observation of a new particle in the search for the Standard Model Higgs boson with the ATLAS detector at the LHC, *Phys. Lett. B* 716 (2012) 1–29. [arXiv:1207.7214](#), [doi:10.1016/j.physletb.2012.08.020](#).
- [3] S. Chatrchyan, et al., Observation of a new boson at a mass of 125 GeV with the CMS experiment at the LHC, *Phys. Lett. B* 716 (2012) 30–61. [arXiv:1207.7235](#), [doi:10.1016/j.physletb.2012.08.021](#).
- [4] S. Chatrchyan, et al., Study of the Mass and Spin-Parity of the Higgs Boson Candidate Via Its Decays to Z Boson Pairs, *Phys. Rev. Lett.* 110 (2013) 081803. [arXiv:1212.6639](#), [doi:10.1103/PhysRevLett.110.081803](#).
- [5] L. D. Landau, On the angular momentum of a system of two photons, *Dokl. Akad. Nauk Ser. Fiz.* 60 (2) (1948) 207–209. [doi:10.1016/B978-0-08-010586-4.50070-5](#).
- [6] C.-N. Yang, Selection Rules for the Dematerialization of a Particle Into Two Photons, *Phys. Rev.* 77 (1950) 242–245. [doi:10.1103/PhysRev.77.242](#).
- [7] S. Moretti, Variations on a Higgs theme, *Phys. Rev. D* 91 (1) (2015) 014012. [arXiv:1407.3511](#), [doi:10.1103/PhysRevD.91.014012](#).
- [8] S. Dawson, S. Dittmaier, M. Spira, Neutral Higgs boson pair production at hadron colliders: QCD corrections, *Phys. Rev. D* 58 (1998) 115012. [arXiv:hep-ph/9805244](#), [doi:10.1103/PhysRevD.58.115012](#).
- [9] S. L. Glashow, S. Weinberg, Natural Conservation Laws for Neutral Currents, *Phys. Rev. D* 15 (1977) 1958. [doi:10.1103/PhysRevD.15.1958](#).
- [10] E. Paschos, Diagonal Neutral Currents, *Phys. Rev. D* 15 (1977) 1966. [doi:10.1103/PhysRevD.15.1966](#).
- [11] J. Bernon, J. F. Guion, H. E. Haber, Y. Jiang, S. Kraml, Scrutinizing the alignment limit in two-Higgs-doublet models. II.  $m_H=125\text{GeV}$ , *Phys. Rev. D* 93 (3) (2016) 035027. [arXiv:1511.03682](#), [doi:10.1103/PhysRevD.93.035027](#).
- [12] D. Eriksson, J. Rathsman, O. Stål, 2HDMC: Two-Higgs-Doublet Model Calculator Physics and Manual, *Comput. Phys. Commun.* 181 (2010) 189–205. [arXiv:0902.0851](#), [doi:10.1016/j.cpc.2009.09.011](#).
- [13] K. Olive, et al., Review of Particle Physics, *Chin. Phys. C* 38 (2014) 090001. [doi:10.1088/1674-1137/38/9/090001](#).
- [14] F. Mahmoudi, SuperIso v2.3: A Program for calculating flavor physics observables in Supersymmetry, *Comput. Phys. Commun.* 180 (2009) 1579–1613. [arXiv:0808.3144](#), [doi:10.1016/j.cpc.2009.02.017](#).
- [15] G. Aad, et al., Combined Measurement of the Higgs Boson Mass in  $pp$  Collisions at  $\sqrt{s} = 7$  and 8 TeV with the ATLAS and CMS Experiments, *Phys. Rev. Lett.* 114 (2015) 191803. [arXiv:1503.07589](#), [doi:10.1103/PhysRevLett.114.191803](#).
- [16] P. Bechtle, S. Heinemeyer, O. Stål, T. Stefaniak, G. Weiglein, *HiggsSignals*: Confronting arbitrary Higgs sectors with measurements at the Tevatron and the LHC, *Eur. Phys. J. C* 74 (2014) 2711. [arXiv:1305.1933](#), [doi:10.1140/epjc/s10052-013-2711-4](#).
- [17] P. Bechtle, O. Brein, S. Heinemeyer, G. Weiglein, K. E. Williams, *HiggsBounds*: Confronting Arbitrary Higgs Sectors with Exclusion Bounds from LEP and the Tevatron, *Comput. Phys. Commun.* 181 (2010) 138–167. [arXiv:0811.4169](#), [doi:10.1016/j.cpc.2009.09.003](#).
- [18] P. Bechtle, O. Brein, S. Heinemeyer, G. Weiglein, K. E. Williams, *HiggsBounds 2.0.0*: Confronting Neutral and Charged Higgs Sector Predictions with Exclusion Bounds from LEP and the Tevatron, *Comput. Phys. Commun.* 182 (2011) 2605–2631. [arXiv:1102.1898](#), [doi:10.1016/j.cpc.2011.07.015](#).
- [19] P. Bechtle, O. Brein, S. Heinemeyer, O. Stål, T. Stefaniak, et al., Recent Developments in *HiggsBounds* and a Preview of *HiggsSignals*, *PoS CHARGED2012* (2012) 024. [arXiv:1301.2345](#).
- [20] P. Bechtle, O. Brein, S. Heinemeyer, O. Stål, T. Stefaniak, et al., *HiggsBounds – 4*: Improved Tests of Extended Higgs Sectors against Exclusion Bounds from LEP, the Tevatron and the LHC, *Eur. Phys. J. C* 74 (2014) 2693. [arXiv:1311.0055](#), [doi:10.1140/epjc/s10052-013-2693-2](#).
- [21] G. Abbiendi, et al., Search for Charged Higgs bosons: Combined Results Using LEP Data, *Eur. Phys. J. C* 73 (2013) 2463. [arXiv:1301.6065](#), [doi:10.1140/epjc/s10052-013-2463-1](#).
- [22] J. Abdallah, et al., Search for fermiophobic Higgs bosons in final states with photons at LEP 2, *Eur. Phys. J. C* 35 (2004) 313–324. [arXiv:hep-ex/0406012](#), [doi:10.1140/epjc/s2004-01869-2](#).
- [23] G. Aad, et al., Search for Higgs bosons decaying to  $aa$  in the  $\mu\mu\tau\tau$  final state in  $pp$  collisions at  $\sqrt{s} = 8$  TeV with the ATLAS experiment, *Phys. Rev. D* 92 (5) (2015) 052002. [arXiv:1505.01609](#), [doi:10.1103/PhysRevD.92.052002](#).
- [24] S. Chatrchyan, et al., Search for Higgs Decays to New Light Bosons in Boosted Tau Final States, Report No. CMS-PAS-HIG-14-022.
- [25] S. Chatrchyan, et al., Search for exotic decays of the Higgs boson to a pair of new light bosons with two muon and two b jets in final states, Report No. CMS-PAS-HIG-14-041.
- [26] S. Chatrchyan, et al., Search for the exotic decay of the Higgs boson to two light pseudoscalar bosons with two taus and two muons in the final state at  $\sqrt{s} = 8$  TeV, Report No. CMS-PAS-HIG-15-011.
- [27] G. Aad, et al., Search for charged Higgs bosons decaying via  $H^\pm \rightarrow \tau^\pm\nu$  in fully hadronic final states using  $pp$  collision data at  $\sqrt{s} = 8$  TeV with the ATLAS detector, *JHEP* 03 (2015) 088. [arXiv:1412.6663](#), [doi:10.1007/JHEP03\(2015\)088](#).
- [28] V. Khachatryan, et al., Search for a charged Higgs boson in  $pp$  collisions at  $\sqrt{s} = 8$  TeV, *JHEP* 11 (2015) 018. [arXiv:1508.07774](#), [doi:10.1007/JHEP11\(2015\)018](#).
- [29] V. Khachatryan, et al., Search for a light charged Higgs boson decaying to  $c\bar{s}$  in  $pp$  collisions at  $\sqrt{s} = 8$  TeV, *JHEP* 12 (2015) 178. [arXiv:1510.04252](#), [doi:10.1007/JHEP12\(2015\)178](#).
- [30] A. Arhrib, R. Benbrik, R. Enberg, W. Klemm, S. Moretti, S. Munir, in progress.
- [31] S. Schael, et al., Search for neutral MSSM Higgs bosons at LEP, *Eur. Phys. J. C* 47 (2006) 547–587. [arXiv:hep-ex/0602042](#), [doi:10.1140/epjc/s2006-02569-7](#).
- [32] J. Alwall, R. Frederix, S. Frixione, V. Hirschi, F. Maltoni, O. Mattelaer, H. S. Shao, T. Stelzer, P. Torrielli, M. Zaro, The automated computation of tree-level and next-to-leading order differential cross sections, and their matching to parton shower simulations, *JHEP* 07 (2014) 079. [arXiv:1405.0301](#), [doi:10.1007/JHEP07\(2014\)079](#).
- [33] B. Hespel, D. Lopez-Val, E. Vryonidou, Higgs pair production via gluon fusion in the Two-Higgs-Doublet Model, *JHEP* 09 (2014) 124. [arXiv:1407.0281](#), [doi:10.1007/JHEP09\(2014\)124](#).
- [34] A. G. Akeroyd, Three body decays of Higgs bosons at LEP-2 and application to a hidden fermiophobic Higgs, *Nucl. Phys. B* 544 (1999) 557–575. [arXiv:hep-ph/9806337](#), [doi:10.1016/S0550-3213\(98\)00845-1](#).